ACS APPLIED MATERIALS & INTERFACES

Research Article

www.acsami.org

A Simple Gas–Solid Route To Functionalize Ordered Carbon

Meherzad F. Variava,* Tamara L. Church, Agus Husin, Andrew T. Harris, and Andrew I. Minett*

Laboratory for Sustainable Technology, School of Chemical and Biomolecular Engineering, The University of Sydney, New South Wales, 2006, Australia

Supporting Information

ABSTRACT: The reaction of nitric oxide (NO) and carbonaceous materials generates nitrogen functionalities on and in graphitic carbons and oxidizes some of the carbon. Here, we have exploited these phenomena to provide a novel route to surface-functionalized multiwalled carbon nanotubes (MWCNTs). We investigated the impacts of NO on the physical and chemical properties of industrially synthesized multiwalled carbon nanotubes to find a facile treatment that increased the specific surface area (S_{BET}) of the MWCNTs by ~20%, with only a minimal effect on their degree of graphitization. The technique caused less material loss (~12 wt %) than traditional gas-based activation techniques and grafted some nitrogen functional groups (1.1 at. %) on the MWCNTs. Moreover, we found that Ni nanoparticles deposited on NO-treated MWCNTs had a crystallite size of d_{Ni} = 13.1 nm, similar to those deposited on acid-treated MWCNTs (d_{Ni} = 14.2 nm), and clearly much smaller than those deposited under the same conditions on untreated MWCNTs (d_{Ni} = 18.3 nm).

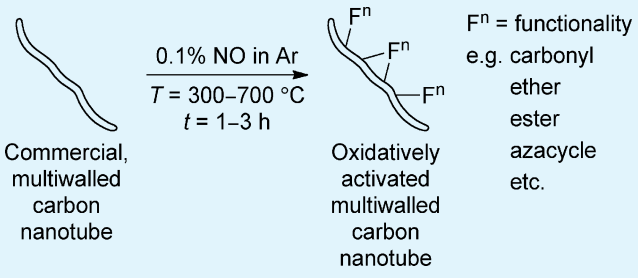

KEYWORDS: *NO oxidation, gas functionalization, CNT oxidation, MWCNTs*

INTRODUCTION

The 1991 "rediscovery"[1] of carbon nanotubes (CNTs)[2] made them the focus of numerous studies.[3−5] Their excellent mechanical, electrical, and thermal properties[6] make them applicable in the fields of energy storage,[7,8] high-strength materials,[9] and catalysis,[10,11] to name a few. CNTs often must be functionalized with metals or polymers in order to be applied. Critical to functionalization is an activation treatment that introduces surface groups, thus converting the relatively inert and hydrophobic surface to a more reactive and hydrophilic one.[4,12,13] The surface activation of CNTs increases their solubility (and, consequently, dispersion in solvents)[14−16] and chemical reactivity,[17,18] as well as their specific surface area,[19,20] all of which facilitate the homogeneous dispersion of nanoparticles within the CNT matrix. Activation treatments are particularly important in the deposition of functional nanoparticles using wetness impregnation, which is a popular method[21−23] that is highly dependent on the dispersion and wettability of the CNT surface. However, covalent activation introduces auxiliary structural defects and thus alters the mechanical and electronic properties of the CNTs, consequently affecting their structural performance.[4,12,13] Thus, when CNTs are used as support materials, the physical characteristics of deposited metal nanoparticles are very closely linked to the method and duration of CNT activation.[24−26] Often, CNTs are activated under oxidizing conditions. For example, inorganic acids[19,27] and other aqueous oxidants (H_2O_2, $KMnO_4$, etc.)[28,29] are used to introduce surface oxygenated groups, mainly carbonyls, carboxyls, and hydroxyls.[27,30] Very few gas–solid oxidizing methods have been reported; those that are known involve oxidizing gases (O_2 and CO_2).[19,20,31] We focused on the gas-phase activation of multiwalled carbon nanotubes (MWCNTs), because such methods are scalable and operationally simple, especially on a large scale, and because they circumvent two major (and energy-consuming) steps that are required after liquid-based activations: filtration and subsequent drying. These cause material losses, as well as MWCNT agglomerations that need further processing (milling or grinding) to redistribute. Moreover, MWCNTs are synthesized on a large scale, generally in fluidized beds (via chemical vapor deposition (CVD)),[32] at temperatures higher than 600 °C. Gas-phase activation can thus be easily implemented downstream of the synthesis during cooling or in a secondary fluidized bed. However, although activation with air, O_2, or CO_2 introduces significantly more surface oxygenated groups and gives a higher specific surface area than common aqueous activation techniques, it is highly detrimental to the structural integrity of the CNTs and gives a lower yield (<60%).[19,20,33] Also, it has been noted that very few carboxyl groups are produced due to the paucity of hydrogen atoms within the system.[34] Ideally, a CNT activation method should not cause excessive material losses (not >30%), but should increase the specific surface area (SSA) while grafting a high amount of oxygenated surface groups (10−15 at. %). Oxygenated groups introduced during the surface activation of CNTs have proven conducive to further chemical functionalization.[23,35] Thus, a milder gaseous oxidant for CNTs could be of significant practical use.

Received: December 1, 2013
Accepted: February 4, 2014
Published: February 4, 2014

Recently, NO_2 (5 vol % in He) has been used to functionalize CNTs.[36] However, that method included a 12-h pretreatment of the CNTs with HCl(*aq*),[36] so the treatment did not circumvent the complex liquid-based purification/functionalization procedure (vide supra). Here, we study the chemical oxidation of MWCNTs by nitric oxide (NO, the major component of NO_x[37,38]), which is an industrial pollutant that is produced in large amounts, at a concentration similar to that found in industrial effluent streams (1200 ppm).[39,40] While studying CNT-supported catalysts, we noted that MWCNTs that were subjected to a NO atmosphere underwent morphological and chemical changes. Furthermore, NO oxidizes carbonaceous substrates,[41,42] and could therefore be used to introduce oxygenated groups at a CNT surface. We endeavored to quantify this effect in terms of surface functional groups and material properties. Thus, we evaluated the potential of NO, an industrial effluent, to serve as a mild, gaseous agent to activate MWCNT surfaces.

EXPERIMENTAL SECTION

NO Activation of Multiwalled Carbon Nanotubes. MWCNTs (>97% carbon content, SW*e*NT SMW100, approximate diameter of 6−9 nm, 90% of tubes have d < 12.2 nm), argon (5.0, Coregas) and NO (0.12% in argon, Coregas) were used as received. A NO concentration of [NO] = 0.12% was chosen to approximate its concentration in industrial effluent streams.[39,40] A single-zone horizontal tube furnace (Model OTF-1200X, MTI) fitted with a quartz tube (ID = 44 mm, length = 500 mm) was employed for the activation studies (see Figure S1 in the Supporting Information). A thin layer of MWCNTs (∼100 mg) was placed in a ceramic boat in the heated zone. Gas flow was controlled via a mass-flow controller (Alicat Scientific). The quartz tube was purged with argon (500 sccm, 20 min) before NO (500 sccm) was introduced and the furnace was heated to the desired temperature (300−700 °C) over 10 min; thus, the heating rate varied (30−70 °C min^{-1}), but all samples had the same duration of NO exposure. Following the heating period, the system was held at the chosen temperature for 1−3 h. After the hold time, the furnace (but not the furnace tube) was opened and quickly cooled to 150 °C (for the reaction at 700 °C, this took 4 min), and the gas was subsequently switched to argon (500 sccm) and allowed to flow for 2 h in order to expel any adsorbed gases (such as NO, N_2, and CO_2).

The oxidation of MWCNTs by NO was also studied gravimetrically using a previously described apparatus.[43] Briefly, a small quantity (∼5 mg) of MWCNTs was heated (15−35 °C min^{-1}) under NO atmosphere (0.1% in Ar, 60 mL min^{-1}) to the required temperature (300−700 °C) in a thermogravimetric analyzer with an attached evolved gas accessory (Model EG-TGA Q500, TA Instruments). The furnace was subsequently held (50 min) at the desired temperature, with NO still flowing, while the sample mass was monitored continuously. The heating rate was chosen according to the target temperature to keep a constant NO-exposure time of 70 min.

Comparison of Activation Methods Using Ni Deposition. NO-treated MWCNTs (700 °C, 1 h, vide supra) were compared to traditional acid-treated MWCNTs (concentrated HNO_3(*aq*), 100 °C, 6 h) to examine the effect of the activation method on their downstream functionalization with Ni. Thus, three samples of MWCNTs (as-received, acid-treated, and NO-treated) were homogeneously dispersed under high-power sonication in separate ethanol aliquots (Absolute, BioLab). $Ni(NO_3)_2{\cdot}6H_2O$ was dissolved in minimal amounts of ethanol, and the resulting solutions were added to the MWCNT dispersions. The mixtures were then dried overnight under continuous stirring (90 °C) before the dried powders were collected and further dried in an oven (120 °C, 4 h). Finally, the impregnated MWCNTs were calcined (10 °C min^{-1} to 500 °C, 2 h hold) under flowing Ar (100 sccm). The final theoretical nickel content of the composites (Ni/MWCNTs) was 15 wt %.

Characterization Techniques. All activated MWCNTs were characterized by N_2 adsorption−desorption and thermogravimetric analysis (TGA), as well as by Raman and X-ray photoelectron spectroscopy (XPS). The specific surface areas (Brunauer−Emmett−Teller,[44] S_{BET}) were calculated over P/P_0 = 0.05−0.35 from N_2 adsorption−desorption isotherms acquired at −196 °C on a sorption apparatus (Autosorb iQ, Quantachrome). Samples were degassed (100 °C, 6 h) prior to analysis. For TGA, the sample (∼5 mg) was heated at 10 °C min^{-1} to 1000 °C under instrument air (60 mL min^{-1}) in a EG-TGA (Model Q500, TA Instruments). Raman spectra were recorded with a Raman spectrometer (InVia, Renishaw) using an Ar^+ ion laser (maximum power = 15 mW) at λ = 514.5 nm (10% laser power, 10 accumulations, ∼10 locations per sample). XPS was carried out on an ESCALAB250Xi spectrometer (Thermo Scientific) at $<2 \times 10^{-9}$ mbar, with monochromatized Al Kα X-rays (1486.68 eV) as the excitation source. In addition to the broad-range spectrum, narrow-scan photoelectron spectra (at 20 eV, spot size 0.5 mm) were recorded for O 1s, C 1s, and N 1s. Spectra were subsequently deconvoluted and peak-fitted (Avantage Software, Thermo Scientific), and elemental concentrations were calculated from detection-sensitivity-adjusted peak areas. Finally, the crystalline structures of the Ni/MWCNTs were evaluated by X-ray diffraction (XRD) (Siemens, Model D5000, 2θ = 20°−70°, interval = 0.0016°, dwell = 10 s) using Cu Kα X-rays (λ = 0.1542 nm). The crystallite size was calculated from the full-width at half-maximum and positions of the peaks using the Scherrer equation.[45]

RESULTS AND DISCUSSION

NO-Treated MWCNTs. To date, most studies involving the oxidation of carbon nanotubes by NO have been focused on maximizing NO conversion (to N_2) rates as a mitigation technology; although NO is also expected to activate the surface of the MWCNTs, there have been few descriptions of the effect.[42,46] In fact, NO has the potential to be an excellent CNT-oxidizing agent, because it oxidizes carbon more slowly[41,47] than other gaseous reagents, such as CO_2 and air.[48,49]

Of the reactions that are reported to occur during the oxidation of C by NO,[47,50,51] eqs 1−3 are of major interest for surface activation:

$$C + xNO \rightarrow CO_x + 0.5xN_2 \quad (1)$$

$$2C() + NO \rightarrow C(N) + C(O) \quad (2)$$

$$C(N) + NO \rightarrow C(O) + N_2 \quad (3)$$

Here, "C()" denotes an active site and C(N) and C(O) represent active, surface-bound nitrogens and oxygens, respectively. In this work, commercial MWCNTs were treated in a NO atmosphere (0.1% in Ar) using a chemical vapor deposition (CVD) apparatus (see Figure S1 in the Supporting Information), and then subjected to physical and chemical analysis. The aim was to map the effects of NO treatment temperature and duration on the MWCNTs, and therefore to find conditions under which oxidation with dilute NO was a useful method for functionalizing the MWCNT surface. First, TGA (Figure S2 in the Supporting Information) was employed to ascertain the extent of chemical damage to the structure of the MWCNTs. The temperature at maximum oxidation rate, which is a measure of MWCNT stability, decreased (Figure 1a) as the NO-oxidation temperature increased. At the same time, the full-width at half-maximum (fwhm) of the largest TGA peak, which is an indicator of the inhomogeneity of carbon species, increased with increasing NO-oxidation temperature. It is likely that the ∼50 °C decrease in temperature at maximum oxidation rate and the ∼25 °C increase in the peak breadth (see

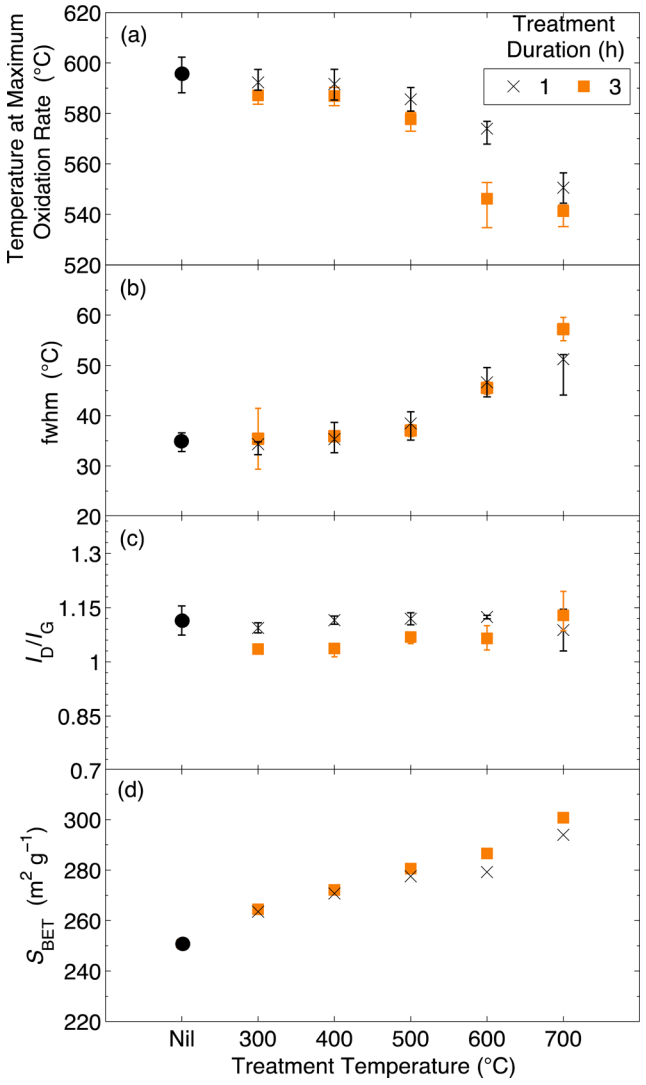

Figure 1. Effects of NO (0.1% in Ar) oxidation on MWCNT properties as functions of temperature and treatment duration: (a) temperature at maximum oxidation rate (60 mL min^{-1} air, dT/dt = 10 °C min^{-1}); (b) full-width at half-maximum (fwhm) of the oxidation peak in panel (a); (c) ratio of the peak intensities of the Raman D- and G-bands (I_D/I_G); and (d) specific surface area (S_{BET}, measured over P/P_0 = 0.05−0.35 at −196 °C) of the MWCNTs. In this figure, solid black circles (●) represent data from as-received MWCNTs; error bars depict the range of values over ≥5 measurements.

Figures 1a and 1b) were caused by a slight increase in nongraphitic surface carbon (e.g., carbon bonded to oxygen) that resulted from the NO-oxidation treatment, as oxidations induce damage and introduce reactive groups to the MWCNT walls.[19,52] This was supported by X-ray photoelectron spectroscopy (XPS), as discussed later.

The impact of the NO treatment on MWCNT graphitization was also examined using Raman spectroscopy (see Figure S3 in the Supporting Information). As-received MWCNTs displayed the two intense Raman peaks that are typical of CNT samples (see Figure S14 in the Supporting Information): the D-band at 1340 cm^{-1}, attributed to defects and disorder in the walls of the MWCNTs, and the G-band at 1590 cm^{-1}, attributed to the C−C stretching mode of graphitic carbon.[53,54] The intensity ratio of the peaks (I_D/I_G) indicates the degree of disorder (or the inverse of the degree of graphitization) in the walls of the MWCNTs.

The I_D/I_G of the as-received MWCNTs ranged from 1.10 to 1.15. These values are common for purified MWCNTs, and indicate fair crystallinity.[55] The average I_D/I_G ratios of the treated materials remained within this range, which indicated that the treatment did not significantly affect the crystallinity of the nanotubes, in contrast to treatments using other gas and physical activation techniques.[19] Although a recent report[56] suggested that Raman spectroscopy can be insensitive to functionalization (specifically acid oxidation) on less-ordered carbon materials, that inference was made based on observations following oxidation under unusually mild conditions (concentrated $H_2SO_4(aq)$ and $HNO_3(aq)$, ~60 °C, 15 min).

N_2-physisorption studies offered further information regarding the effect of NO-based activation on the MWCNTs. N_2 adsorption−desorption isotherms of both the as-received and the NO-treated MWCNTs were IUPAC Type-II (see Figure S17a in the Supporting Information).[57] The hysteresis observed at high relative pressures, likely caused by the condensation of N_2 in the interstices between individual MWCNTs,[58] indicated a pore structure with mesoporous features,[59] in agreement with published research.[22,60] However, the isotherms could not be considered Type IV, which is characteristic of mesoporous materials, as no horizontal plateau was seen at high relative pressure.[59] The specific surface area (S_{BET}) of the MWCNTs increased from 250 m^2 g^{-1} (±8 m^2 g^{-1}, calculated following analysis of five samples from the same 1-kg batch supplied by SWeNT) for as-synthesized MWCNTs (in agreement with a previously published report[61]) up to 300 m^2 g^{-1} at the highest treatment temperature. This indicated the oxidation of carbons within MWCNTs as well as the grafting of functional groups (Figure 2), both of which increase the porosity and surface area of CNTs.[19,62] The size of ΔS_{BET} observed (20%) is comparable to those reported following other gas activations.[19,20,62,63] Furthermore, neither surface area nor weight loss was significantly dependent on treatment time. This, in agreement with TGA analysis, suggested that treatment longer than 1 h was unnecessary for the introduction of functionalities to the MWCNTs structure. Also, very little N_2 was adsorbed at low relative pressure (at P/P_0 = 0.05, 57 and 64 cm^3 g^{-1} of N_2 was adsorbed on as-received MWCNTs and those treated for 3 h at 700 °C, respectively (see Figures S17a and S17b in the Supporting Information), indicating that significant micropores[59] were neither present in the as-synthesized MWCNTs nor developed upon activation with NO.

The surface compositions of the activated MWCNTs were studied by XPS. This technique was considered representative of the MWCNT surface throughout the system, as a wide beam spot size (500 μm) was used and the MWCNTs were present as large agglomerates. Consistent with the Raman spectroscopic results, the C 1s core level XPS spectrum of the NO-treated MWCNTs (0.1% NO in Ar, 700 °C, 3 h) confirmed the significant presence of C═C bonds (see Figure S18 in the Supporting Information), where the binding energy (BE) of 284.3 eV is characteristic of graphitic carbon bonds in MWCNTs.[64] Deconvolution of the C 1s core level spectrum (see Figure S18 in the Supporting Information) also indicated the presence of other types of carbon atoms. Significantly, sp^3-hybridized C bonds (defects, BE = 285.3 eV), as well as both sp^3- and sp^2-hybridized carbons bonded to oxygen (≡C*−O, BE = 286.8 eV; >C*═O, BE = 288.2 eV; −O−C*═O, BE =

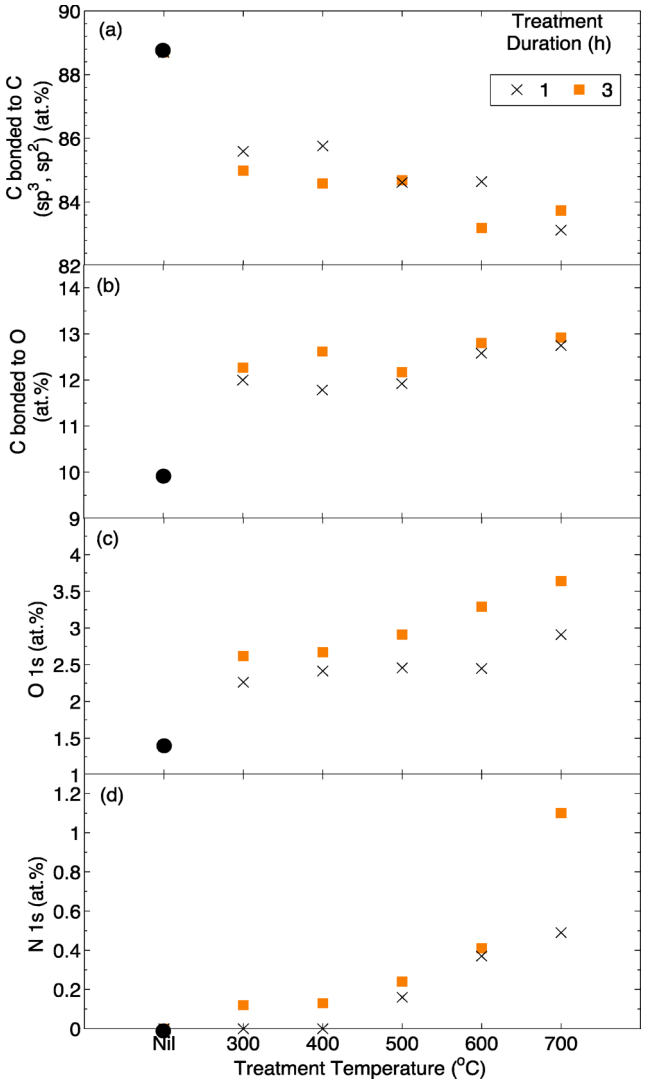

Figure 2. Effect of NO (0.1% in argon) oxidation on MWCNT surface composition as a function of temperature and treatment duration, as determined from XPS investigations; panels show the effect on content of (a) carbon bonded to carbon (sp^2 and sp^3), (b) carbon bonded to oxygen, (c) oxygen, and (d) nitrogen. For assignments, see Figure S18 in the Supporting Information. Note that, in this figure, the solid circle (●) represent data from as-received MWCNTs.

289.2 eV) were present on the activated MWCNTs.[27,30,64] This was further confirmed by the O 1s core level spectra of the NO-activated CNTs (see Figures S5 and S6 in the Supporting Information), which displayed major contributions from oxygen atoms that were doubly (O*═C, BE = 531.5 eV) and singly (O*−C, BE = 533.2 eV) bonded to carbon.[64,65] Singly bonded oxygen is likely to be introduced as ethers,[66] rather than as phenols or other hydroxyls, given that no source of H atoms was added during the treatments. However, it is difficult to rule out the formation of hydroxyls or phenols via the hydrolysis of ethers or epoxides upon exposure to air prior to the ex situ XPS studies. In any case, the lack of introduced H atoms suggests that the doubly bonded O atoms are unlikely to be present as aldehydes. In addition, aldehydes are unstable at even the lowest treatment temperature (300 °C),[67] and would decompose if formed. Thus, compared to common acid-based activation techniques (i.e., those using $HNO_3(aq)$, $H_2SO_4(aq)$, or mixtures of the two), where the dominant surface oxygenated carbon groups are carboxyl and hydroxyl groups (>40 at. % of the oxygen that is bound to carbon[27,68]), the activation of MWCNTs with NO primarily produces carbon doubly bound to oxygen (>70 at. %; see Figures S5 and S6 in the Supporting Information).

Furthermore, any esters, anhydrides, and pyrones would contribute to both deconvoluted peaks in the O 1s core-level spectra, as they contain O atoms in two distinct electronic environments, i.e., those with primarily C−O and primarily C═O character.[34] The slightly higher intensity of the "C*−O" peak within the C 1s spectra (see Figure S18 in the Supporting Information) than the C−O* peak in the O 1s spectra can be explained by the likely presence of carbons bound to nitrogen. C*−N peaks occur from 285 eV to 286.5 eV in C 1s spectra;[69,70] however, the relative C*−O and C*−N contributions to the C 1s peaks in this system are hard to allocate because of the low N content of the sample (1.5 wt %). In any case, given that the oxidation method involved heating the MWCNTs with a reactive nitrogen species, we examined the N 1s species on the as-received and treated MWCNTs. Indeed, both pyridinic and graphitic N atoms (BE = 398.6 and 400.3 eV, respectively) were detected on the latter sample.[65] The N content (1.5 wt %; see Figure 2) was lower than that commonly observed in N-doped MWCNTs,[71] making this a feasible post-synthesis route to MWCNTs with low N contents. Quantitatively, raising the temperature of the NO activation treatment increased the amounts of both oxygen and nitrogen on the MWCNT surfaces (Figure 2). However, as tempting it may be to analyze the variations in N species (i.e., pyridinic and graphitic) with respect to temperature, the low concentration of nitrogen in the MWCNT samples prohibits reliable analysis. Note that, for all XPS data, the small (<0.1 eV) differences between the measured and reported BEs are within the range of variation that can be caused by surface charge compensation.[65,72] Because of overlapping peaks (see Figure S18 in the Supporting Information) present in the core XPS spectra and the ambiguity of peak deconvolution, we hesitate to comment on the relative concentrations of individual functional groups (e.g., singly vs doubly bound oxygen), except in the case of the well-resolved peak for carbon bonded to carbon (sp^2 and sp^3, vide supra). Clearly, however, both N and O were added to the MWCNT surfaces, even at 300 °C (albeit when treated for 3 h). The degree of functionalization increased somewhat at higher temperatures, and the N content increased dramatically upon extended treatment at 700 °C.

Loss of MWCNT Mass during NO Treatment. Of course, to investigate the potential destructive impact of this activation method on the MWCNTs, we tested the loss of MWCNT material during treatment. As-received MWCNTs were tested using a previously described gravimetric apparatus (see Experimental Methods).[43] When heated under a flow of 0.12% NO in Ar at 600 or 700 °C, the MWCNTs underwent monotonic weight loss, with the rate of material loss depending on the treatment temperature (Figure 3). Under the most severe treatment (700 °C, 1 h; see Figure 3), the sample mass decreased by ∼20 wt %. This was significantly less than for other gas activation treatments, where >40% material losses have been reported.[19,20,33] NO-activation at 300 or 400 °C resulted in a minimal loss of material that was not time-dependent after the initial heating period, suggesting that longer heating periods under these conditions could be exploited to functionalize CNTs with little material loss. At 500 °C, mass loss was slow but measurable throughout the

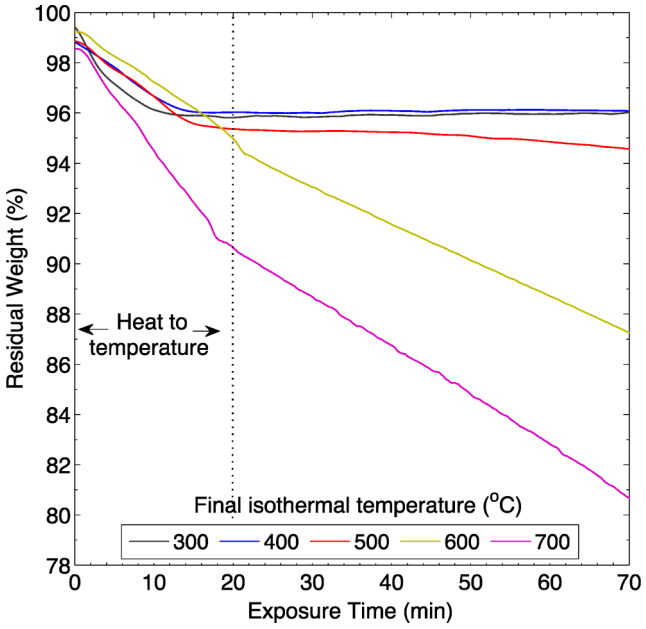

Figure 3. Mass of MWCNTs as a function of duration of exposure to NO (0.1% in argon). The dashed line illustrates the end of the heating period and the beginning of the isothermal step (at the relevant temperature). See the Experimental Methods section for further details.

reaction time. These results are in agreement with previous research,[46,51,73] which has shown that the reaction between carbon and NO is initiated at ~500−600 °C. The minimal decomposition we observed at lower temperatures (300−500 °C, Figure 3) was likely due to the oxidation of amorphous carbon in the MWCNT matrix, as this is more reactive than graphitic tubules.[74] Furthermore, it could be caused by the reaction of adsorbed atmospheric oxygen with amorphous carbon at these temperatures;[46] however, this should be limited as the experiments were conducted in argon. Finally, it could be attributed to the reaction of functional groups/nongraphitic defect sites with NO; this is known to occur at temperatures higher than 200 °C.[36,47] Treatment in NO at 300 °C for as little as 5−10 min (Figure 3) was sufficient to oxidize all of the reactive amorphous carbon and defect sites, as was simply heating to 400 °C under NO; as a result, the samples treated at 300 and 400 °C had very similar properties (see Figures 1 and 2), and lost little mass upon extended heating (Figure 3). The functional groups introduced under these conditions were likely concentrated at the edges of the graphitic regions of the materials, although this could not be confirmed by XPS at the low rates of N and O incorporation produced. At higher temperatures, NO reacted with the graphitic carbon at rates that increased with temperature, causing continuous mass loss; this was quite slow at 500 °C. This reaction between NO and graphitic carbon was more rapid at 600 and 700 °C, where it caused a faster degradation of the samples (Figure 3), as well as larger increases in their N and O contents, at the expense of carbon−carbon bonds (Figure 2). Thus, this technique offers a choice between the slow evolution of surface functionalities at lower temperatures, and faster evolution at higher temperatures, but at a (still modest) cost in MWCNTs.

Effect of Activation Treatment on Ni Deposition. Carbons (CNTs, activated, graphene, etc.) are generally activated in order to improve their dispersion characteristics, as well as to increase their reactive-surface-site content. The latter allows the material to support smaller, better-dispersed functional metal nanoparticles.[25,75] Thus, we compared our treated MWCNTs to traditionally acid-activated MWCNTs by supporting nickel on their surfaces. Supported nickel composites catalyze a range of hydrogenation and dehydrogenation reactions,[76] and are thus particularly interesting for industrial implementation. Nickel particles were supported on untreated, NO-treated, and acid-treated MWCNTs, and the crystallite structures of Ni in the products were investigated using X-ray diffraction (XRD), from which the mean crystallite (not particle) size of a species within a bulk material can be calculated. The XRD patterns (Figure 4) of all three Ni/

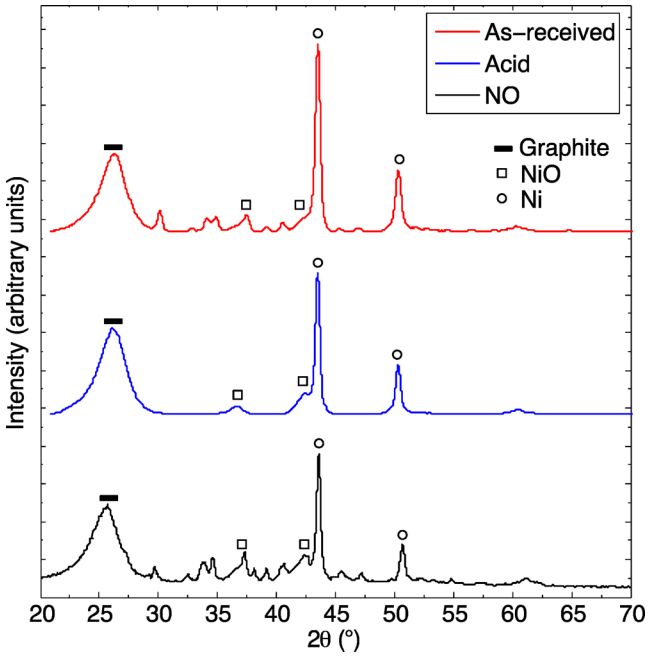

Figure 4. X-ray diffraction (XRD) patterns of Ni/MWCNTs (15 wt % nickel) produced on as-received, acid-treated, and NO-treated MWNCTs. Indicated phases are indicated as follows: (−) the graphite structure (002) plane of MWCNTs at 26.5°; (□) NiO (JCPDS File Card No. 47-1049) at 37.1° (111), 43.5° (200), and 62.9° (001); and (○) Ni (JCPDS File Card No. 45-1027) at 44.8° (111) and 51.8° (200).

MWCNT samples contained peaks at 44.8° and 51.8°, which were assigned to the (111) and (200) diffraction planes, respectively, of Ni^0 (JCPDS File Card No. 45-1027). This was surprising, as no reducing agent was used, but solid graphitic carbons have been shown to reduce NiO in the past, albeit at temperatures >800 °C,[77,78] and other carbon-containing compounds such as carbon black, polystyrene, and polyethylene reduce Ni^{2+} to Ni^0 at much lower temperatures (340−730 °C).[79] Thus, the MWCNTs are likely responsible for the reduction of Ni^{2+} (introduced as $Ni(NO_3)_2$; see the Experimental Methods section) to Ni^0, either directly (i.e., via charge transfer from the CNT structure) or via the CO (a known reducing agent) formed when the MWCNTs were heated with the oxygen-containing Ni precursor. In any case, it provides a method to deposit Ni^0 on MWCNTs without the help of reducing substances (e.g., $NaBH_4$ or KBH_4) or gases (e.g., CO or H_2). Note, however, that NiO was present as a minor species on the composites (Figure 4), as demonstrated

by small peaks at 37.1°, 43.5°, and 62.9° (attributed to NiO (JCPDS File Card No. 47-1049), with possible contributions from graphitic carbon). The rest of the peaks arose from the proprietary catalysts used to synthesize the MWCNTs; these contain alumina-supported $CoFe_2O_4$, $CoMoO_4$, Co_xMoO_4, $Co_xFe_yMoO_4$, and $Fe_2(MoO_4)_3$.[80] As expected, acid treatment completely removed these residual impurities.[81] The average Ni^0 crystallite size on the MWCNTs, calculated using the Scherrer equation,[45] was 18.3 ± 0.5 nm for as-received MWCNTs, but just 13.1 ± 1.1 nm and 14.2 ± 0.6 nm for acid- and NO-activated MWCNTs, respectively. Thus, the NO treatment had an activation effect akin to that achieved using traditional acid-oxidation technique, but should be far simpler to implement in large-scale CNT manufacturing systems, which are predominantly CVD-based.

CONCLUSION

We have developed a NO-based method to activate multiwalled carbon nanotubes (MWCNTs). As the technique occurs at the gas/solid interface, it can be simply implemented following MWCNT synthesis by chemical vapor deposition (CVD). After activation, the MWCNTs were easily retrieved without additional processing steps like filtration, washing or drying. This limits the number of steps required to produce activated MWCNTs (and therefore any downstream products), thus lowering synthesis costs and opening the door to much wider production capabilities. These advantages make the process extremely appealing for implementation in the large-scale production of N- and O-functionalized MWCNTs with high surface areas. The true test of the activation method was to ensure that it favored the deposition of small, well-dispersed nanoparticles on the MWCNT surfaces, and we thus compared nickel deposition on MWCNTs activated with NO to those activated using a traditional, and energy-intensive, treatment in aqueous acid. Indeed, wet impregnation of NO-treated MWCNTs with $Ni(NO_3)_2{\cdot}6H_2O$ gave nickel nanoparticles similar in size (14.2 nm) to those deposited on acid-treated MWCNTs (13.1 nm); those deposited on untreated MWCNTs were clearly larger (18.3 nm). Interestingly, we found that Ni^0 was the predominant product of functionalization on the MWCNTs following calcination under an inert atmosphere, regardless of activation method; thus, the carbon from the MWCNTs played a role in this reduction. This observation is, to our knowledge, previously unreported, and is expected to be extremely convenient for future CNT-based functionalization.

Further studies are required to ascertain the effects of the NO-based activation treatment in a fluidized bed. Also, various combinations of gases, including diluted steam, can be tested in order to tune the types of heteroatom-containing groups that are grafted onto MWCNTs, thus tailoring the materials for specific applications. In addition, other carbonaceous materials, such as chars and activated carbon, can be used to treat NO/NO_2 effluent streams, either by reduction or adsorption.[41,46,50] Thus, in-depth studies may permit the use of a NO recycle stream that returns off-gases to the MWCNT reactor, allowing this reaction to act as a technology to mitigate NO_x compounds.

ASSOCIATED CONTENT

Supporting Information

Experimental apparatus, TGA curves, Raman spectra, N_2 adsorption−desorption curves, and X-ray photoelectron spectra. This material is available free of charge via the Internet at http://pubs.acs.org.

AUTHOR INFORMATION

Corresponding Authors

*Tel.: +61 2 9114 1446. Fax: +61 2 9351 2854. E-mail: andrew.minett@sydney.edu.au (A. I. Minett).

*Tel.: +61 2 9351 2926. Fax: +61 2 9351 2854. E-mail: meherzad.variava@sydney.edu.au (M. F. Variava).

Author Contributions

The manuscript was written through contributions of all authors. All authors have given approval to the final version of the manuscript.

Notes

The authors declare no competing financial interest.

ACKNOWLEDGMENTS

M.F.V. and A.H. are grateful to the University of Sydney and the Australian Research Council (ARC) for funding this research. A.T.H. and A.I.M. acknowledge the ongoing support of the ARC. The authors acknowledge the facilities and the scientific and technical assistance of the Australian Microscopy & Microanalysis Research Facility node (Sydney Microscopy and Microanalysis) at the University of Sydney, and are grateful to Mr. V. Lo (The University of Sydney) for TEM analysis, Dr. L. Carter (School of Chemistry, The University of Sydney) for her assistance with Raman spectroscopy analysis, Dr. B. Gong (The University of New South Wales Analytical Centre) for his assistance with XPS analysis, and Dr. J. Shi (School of Chemical and Biomolecular Engineering, The University of Sydney) for assistance with N_2 adsorption measurements.

REFERENCES

(1) Iijima, S. *Nature* **1991**, *354*, 56−58.
(2) Iijima, S.; Ichihashi, T. *Nature* **1993**, *363*, 603−605.
(3) Lynam, C.; Minett, A. I.; Habas, S. E.; Gambhir, S.; Officer, D. L.; Wallace, G. G. *Int. J. Nanotechnol.* **2008**, *5*, 331−351.
(4) Variava, M. F.; Church, T.; Harris, A. T.; Minett, A. I. *J. Mater. Chem. A* **2013**, *1*, 8509.
(5) Variava, M. F.; Church, T. L.; Harris, A. T. *Appl. Catal., B* **2012**, *123−124*, 200−207.
(6) Dresselhaus, M. S.; Dresselhaus, G.; Charlier, J. C.; Hernández, E. *Philos. Trans. R. Soc. London, Ser. A* **2004**, *362*, 2065−2098.
(7) Wang, C.; Waje, M.; Wang, X.; Tang, J. M.; Haddon, R. C.; Yan, Y. *Nano Lett.* **2004**, *4*, 345−348.
(8) Chen, J.; Liu, Y.; Minett, A. I.; Lynam, C.; Wang, J. Z.; Wallace, G. G. *Chem. Mater.* **2007**, *19*, 3595−3597.
(9) Calvert, P. *Nature* **1999**, *399*, 210−211.
(10) Zhu, J.; Holmen, A.; Chen, D. *ChemCatChem* **2013**, *5*, 378−401.
(11) Zhang, W.; Sherrell, P.; Minett, A. I.; Razal, J. M.; Chen, J. *Energy Environ. Sci.* **2010**, *3*, 1286−1293.
(12) Balasubramanian, K.; Burghard, M. *Small* **2005**, *1*, 180−192.
(13) Avilés, F.; Cauich-Rodríguez, J. V.; Moo-Tah, L.; May-Pat, A.; Vargas-Coronado, R. *Carbon* **2009**, *47*, 2970−2975.
(14) Tasis, D.; Tagmatarchis, N.; Georgakilas, V.; Prato, M. *Chem.—Eur. J.* **2003**, *9*, 4000−4008.
(15) Rosca, I. D.; Barsan, M. M.; Butler, I. S.; Kozinski, J. A. *Carbon* **2009**, *47*, 2552−2555.
(16) Xing, Y.; Li, L.; Chusuei, C. C.; Hull, R. V. *Langmuir* **2005**, *21*, 4185−4190.
(17) Lu, J. S. *Carbon* **2007**, *45*, 1599−1605.
(18) Hu, J.; Chen, C.; Zhu, X.; Wang, X. *J. Hazard. Mater.* **2009**, *162*, 1542−1550.

(19) Solhy, A.; Machado, B. F.; Beausoleil, J.; Kihn, Y.; Gonçalves, F.; Pereira, M. F. R.; Órfão, J. J. M.; Figueiredo, J. L.; Faria, J. L.; Serp, P. *Carbon* **2008**, *46*, 1194−1207.
(20) Li, C. S.; Wang, D. Z.; Liang, T. X.; Wang, X. F.; Wu, J. J.; Hu, X. Q.; Liang, J. *Powder Technol.* **2004**, *142*, 175−179.
(21) van Steen, E.; Prinsloo, F. F. *Catal. Today* **2002**, *71*, 327−334.
(22) Ovejero, G.; Sotelo, J. L.; Romero, M. D.; Rodríguez, A.; Ocaña, M. A.; Rodríguez, G.; García, J. *Ind. Eng. Chem. Res.* **2006**, *45*, 2206−2212.
(23) Azadi, P.; Farnood, R.; Meier, E. *J. Phys. Chem. A* **2010**, *114*, 3962−3968.
(24) Bahr, J. L.; Tour, J. M. *J. Mater. Chem.* **2002**, *12*, 1952−1958.
(25) Banerjee, S.; Hemraj-Benny, T.; Wong, S. S. *Adv. Mater.* **2005**, *17*, 17−29.
(26) Peng, X. H.; Wong, S. S. *Adv. Mater.* **2009**, *21*, 625−642.
(27) Datsyuk, V.; Kalyva, M.; Papagelis, K.; Parthenios, J.; Tasis, D.; Siokou, A.; Kallitsis, I.; Galiotis, C. *Carbon* **2008**, *46*, 833−840.
(28) Xu, C. L.; Chen, J. F.; Cui, Y.; Han, Q. Y.; Choo, H.; Liaw, P. K.; Wu, D. H. *Adv. Eng. Mater.* **2006**, *8*, 73−77.
(29) Marega, R.; Accorsi, G.; Meneghetti, M.; Parisini, A.; Prato, M.; Bonifazi, D. *Carbon* **2009**, *47*, 675−682.
(30) Stobinski, L.; Lesiak, B.; Kövér, L.; Tóth, J.; Biniak, S.; Trykowski, G.; Judek, J. *J. Alloys Compd.* **2010**, *501*, 77−84.
(31) Tsang, S. C.; Harris, P. J. F.; Green, M. L. H. *Nature* **1993**, *362*, 520−522.
(32) See, C. H.; Harris, A. T. *Ind. Eng. Chem. Res.* **2007**, *46*, 997−1012.
(33) Behler, K.; Osswald, S.; Ye, H.; Dimovski, S.; Gogotsi, Y. *J. Nanopart. Res.* **2006**, *8*, 615−625.
(34) Xia, W.; Jin, C.; Kundu, S.; Muhler, M. *Carbon* **2009**, *47*, 919−922.
(35) Abbaslou, R. M. M.; Tavasoli, A.; Dalai, A. K. *Appl. Catal., A* **2009**, *355*, 33−41.
(36) Chen, C.; Zhang, J.; Peng, F.; Su, D. *Mater. Res. Bull.* **2013**, *48*, 3218−3222.
(37) Gómez-García, M. A.; Pitchon, V.; Kiennemann, A. *Environ. Int.* **2005**, *31*, 445−467.
(38) Bosch, H.; Janssen, F. *Catal. Today* **1988**, *2*, 369−379.
(39) Heck, R. M. *Catal. Today* **1999**, *53*, 519−523.
(40) Epling, W. S.; Campbell, L. E.; Yezerets, A.; Currier, N. W.; Parks, J. E. *Catal. Rev.* **2004**, *46*, 163−245.
(41) Atkinson, J. D.; Zhang, Z.; Yan, Z.; Rood, M. J. *Carbon* **2013**, *54*, 444−453.
(42) Tsang, S. C.; Chen, Y. K.; Green, M. L. H. *Appl. Catal., B* **1996**, *8*, 445−455.
(43) Mackenzie, K. J.; Dunens, O. M.; Harris, A. T. *Carbon* **2013**, *59*, 344−365.
(44) Brunauer, S.; Emmett, P. H.; Teller, E. *J. Am. Chem. Soc.* **1938**, *60*, 309−319.
(45) Scherrer, P. *Nachr. Ges. Wiss. Göttingen* **1918**, *26*, 98−100.
(46) Tighe, C. J.; Dennis, J. S.; Hayhurst, A. N.; Twigg, M. V. *Proc. Combust. Inst.* **2009**, *32*, 1989−1996.
(47) Stanmore, B. R.; Tschamber, V.; Brilhac, J. F. *Fuel* **2008**, *87*, 131−146.
(48) Sietsma, J. R. A.; Meeldijk, J. D.; den Breejen, J. P.; Versluijs-Helder, M.; van Dillen, A. J.; de Jongh, P. E.; de Jong, K. P. *Angew. Chem., Int. Ed.* **2007**, *46*, 4547−4549.
(49) Sietsma, J. R. A.; Friedrich, H.; Broersma, A.; Versluijs-Helder, M.; van Dillen, A. J.; de Jongh, P. E.; de Jong, K. P. *J. Catal.* **2008**, *260*, 227−235.
(50) Chambrion, P.; Kyotani, T.; Tomita, A. *Energy Fuels* **1998**, *12*, 416−421.
(51) Suzuki, T.; Kyotani, T.; Tomita, A. *Ind. Eng. Chem. Res.* **1994**, *33*, 2840−2845.
(52) Hanus, M. J.; King, A. A. K.; Minett, A. I.; Harris, A. T. *Sep. Purif. Technol.* **2012**, *96*, 248−255.
(53) Dresselhaus, M. S.; Dresselhaus, G.; Saito, R.; Jorio, A. *Phys. Rep.* **2005**, *409*, 47−99.
(54) Costa, S.; Borowiak-Palen, E. *Acta Phys. Pol., A* **2009**, *116*, 32−35.
(55) Liu, J.; Dunens, O. M.; Mackenzie, K. J.; See, C. H.; Harris, A. T. *AIChE J.* **2008**, *54*, 3303−3307.
(56) Schönfelder, R.; Avilés, F.; Knupfer, M.; Azamar-Barrios, J. A.; González-Chi, P. I.; Rümmeli, M. H. *J. Exp. Nanosci.* **2013**, 1−11.
(57) Sing, K. S. W.; Everett, D. H.; Haul, R. A. W.; Moscou, L.; Pierotti, R. A.; Rouquerol, J.; Siemieniewska, T. *Pure Appl. Chem.* **1985**, *57*, 603−619.
(58) Inoue, S.; Ichikuni, N.; Suzuki, T.; Uematsu, T.; Kaneko, K. *J. Phys. Chem. B* **1998**, *102*, 4689−4692.
(59) Rouquerol, J.; Rouquerol, F.; Sing, K. S. *Absorption by Powders and Porous Solids*, 1st Edition; Academic Press: London, 1998.
(60) Kim, D. Y.; Yang, C.-M.; Park, Y. S.; Kim, K. K.; Jeong, S. Y.; Han, J. H.; Lee, Y. H. *Chem. Phys. Lett.* **2005**, *413*, 135−141.
(61) Li, Y.; Zhu, J.; Wei, S.; Ryu, J.; Wang, Q.; Sun, L.; Guo, Z. *Macromol. Chem. Phys.* **2011**, *212*, 2429−2438.
(62) Seo, M.-K.; Park, S.-J. *Curr. Appl. Phys.* **2010**, *10*, 241−244.
(63) Zhang, A. M.; Dong, J. L.; Xu, Q. H.; Rhee, H. K.; Li, X. L. *Catal. Today* **2004**, *93*−*95*, 347−352.
(64) Ago, H.; Kugler, T.; Cacialli, F.; Salaneck, W. R.; Shaffer, M. S. P.; Windle, A. H.; Friend, R. H. *J. Phys. Chem. B* **1999**, *103*, 8116−8121.
(65) Okpalugo, T. I. T.; Papakonstantinou, P.; Murphy, H.; Mclaughlin, J.; Brown, N. M. D. *Carbon* **2005**, *43*, 153−161.
(66) Setiabudi, A.; Makkee, M.; Moulijn, J. A. *Appl. Catal., B* **2004**, *50*, 185−194.
(67) Kundu, S.; Wang, Y.; Xia, W.; Muhler, M. *J. Phys. Chem. C* **2008**, *112*, 16869−16878.
(68) Wepasnick, K. A.; Smith, B. A.; Schrote, K. E.; Wilson, H. K.; Diegelmann, S. R.; Fairbrother, D. H. *Carbon* **2011**, *49*, 24−36.
(69) Papakonstantinou, P.; Lemoine, P. *J. Phys.: Condens. Matter* **2001**, *13*, 2971.
(70) Maldonado, S.; Morin, S.; Stevenson, K. J. *Carbon* **2006**, *44*, 1429−1437.
(71) Ayala, P.; Arenal, R.; Rümmeli, M.; Rubio, A.; Pichler, T. *Carbon* **2010**, *48*, 575−586.
(72) Kuivila, C. S.; Butt, J. B.; Stair, P. C. *Appl. Surf. Sci.* **1988**, *32*, 99−121.
(73) Aarna, I.; Suuberg, E. M. *Fuel* **1997**, *76*, 475−491.
(74) Shao, L.; Tobias, G.; Salzmann, C. G.; Ballesteros, B.; Hong, S. Y.; Crossley, A.; Davis, B. G.; Green, M. L. H. *Chem. Commun.* **2007**, 5090−5092.
(75) Hirsch, A. *Angew. Chem., Int. Ed.* **2002**, *41*, 1853−1859.
(76) Leach, B. E. *Applied Industrial Catalysis*, 1st Edition; Academic Press: New York, 1983.
(77) Sharma, S. K.; Vastola, F. J.; Walker, P. L., Jr. *Carbon* **1997**, *35*, 529−533.
(78) Sharma, S. K.; Vastola, F. J.; Walker, P. L., Jr. *Carbon* **1996**, *34*, 1407−1412.
(79) Grigor'yan, E. G.; Niazyan, O. M.; Kharatyan, S. L. *Kinet. Catal.* **2007**, *48*, 773−777.
(80) (a) Prada Silvy, R.; Tan, Y. (Southwest Nanotechnologies, Inc., USA). Pct Int. Pat. WO 2011009071 A1 (*Chem. Abstr.* **2011**, *154*, 168430). (b) Prada Silvy, R.; Culot, B.; Pirlot, C. (Nanocyl S.A., Belgium). Pct Int. Pat. WO 2007033438 A1 (*Chem. Abstr.* **2007**, *146*, 345422).
(81) Mackenzie, K.; Dunens, O.; Harris, A. T. *Sep. Purif. Technol.* **2009**, *66*, 209−222.